Check for updates

Design and fabrication of nano-composite ceramic membranes for the adsorption of antibiotics from pharmaceutical wastewater†

Mohsen Moghimi Dehkordi,[a] Soheila Hedayatikhah,*[b] Mina Haghmohammadi,[c] Mozhgan Amiri Baramkohi,[d] Ali Montazeri[e] and Ali Aghababai Beni [iD] *[f]

Antibiotic contamination in pharmaceutical wastewater poses environmental and public health risks. This study synthesized a nanocomposite ceramic adsorbent from clay, cow bone powder (hydroxyapatite nanoparticles), and human hair for antibiotic removal. The adsorbent exhibited high mechanical strength (3.6 bar), chemical stability, and a large surface area (171.32 m^2 g^{-1}). Characterization (FTIR, XRD, FE-SEM, BET) confirmed successful nanoparticle incorporation. In a vertical fixed-bed column, optimal removal occurred at pH 7, 25 g adsorbent, 25 °C, and 40 min contact time. Adsorption was endothermic, following pseudo-first-order and intraparticle diffusion models. The adsorbent retained >90% efficiency after 142 regeneration cycles, proving its durability and cost-effectiveness.

1. Introduction

The widespread use of antibiotics in medicine, agriculture, and animal husbandry has led to their release into the environment, resulting in significant environmental pollution.[1] Antibiotics are known as emerging pollutants due to their high stability and easy transfer to surface and groundwater. They can have detrimental effects on aquatic ecosystems and human health. Particularly, the emergence of antibiotic resistance in bacteria poses a serious threat to public health, driven by the presence of antibiotics in the environment.[2]

Various antibiotics, including tetracyclines, fluoroquinolones, and sulfonamides, have been identified in water sources across different countries. These pollutants enter the environment not only through industrial and hospital wastewater but also through agricultural activities. Therefore, developing effective materials and technologies to remove antibiotics from contaminated waters is of paramount importance.[3,4]

Several methods exist for removing antibiotics from water, but adsorption has garnered attention as an effective method

due to its high efficiency, low cost, and operational simplicity.[5,6] In this regard, diverse adsorbent materials such as activated carbons, resins, metal oxides, and metal–organic frameworks (MOFs) have been studied.[7,8] These materials have high adsorption capacities due to their large surface areas and porous structures, although each has its limitations.[9,10]

Various methods have been employed to remove antibiotics from industrial and hospital wastewater, each with its own advantages and limitations. Advanced oxidation processes (AOPs), such as photocatalysis and ozonation, can degrade resistant organic compounds into harmless substances; however, their high operational costs and the generation of toxic byproducts remain significant challenges. Membrane processes, including reverse osmosis (RO) and nanofiltration (NF), demonstrate high efficiency in removing pharmaceutical pollutants, but issues such as membrane fouling, high-pressure requirements, and expensive membrane replacement limit their industrial applications. Biological methods, which rely on microbial degradation of antibiotics, are considered environmentally friendly, yet they are typically time-consuming and ineffective for certain persistent compounds. Among these approaches, adsorption has gained significant attention as an efficient, cost-effective, and straightforward method, especially with the development of nanostructured adsorbents that offer high adsorption capacities. However, the primary challenge of using nanoadsorbents is their separation from the medium after the adsorption process, which can lead to environmental concerns. Adsorption has garnered attention as an effective method due to its high efficiency, low cost, and operational simplicity. In this regard, diverse adsorbent materials such as activated carbons, resins, metal oxides, and metal–organic frameworks (MOFs) have been studied. These materials have

[a]*Department of Biochemistry, Faculty of Sciences, Payame Noor University, Isfahan, Iran*

[b]*Department of Chemical Engineering, Mahshahr Branch, Islamic Azad University, Mahshahr, Iran. E-mail: ss.hedayatikhah69@yahoo.com*

[c]*Department of Organic Chemistry, Faculty of Chemistry, University of Semnan, Semnan, Iran*

[d]*Department of Chemistry, Faculty of Science, University of Zanjan, Zanjan, Iran*

[e]*Department of Energy, Materials and Energy Research Center, Karaj, Iran*

[f]*Department of Chemical Engineering, Shahrekord Branch, Islamic Azad University, Shahrekord, Iran. E-mail: aliaghababai@yahoo.com; Tel: +98-9139781836*

† Electronic supplementary information (ESI) available. See DOI: https://doi.org/10.1039/d5ra00414d

high adsorption capacities due to their large surface areas and porous structures, although each has its limitations.

Zhang et al.[11] investigated the efficient adsorption of antibiotics from aqueous solutions using $ZnCl_2$-activated biochar derived from the invasive species *Spartina alterniflora*. The biochar, optimized through high-temperature calcination and $ZnCl_2$ activation, showed enhanced adsorption performance due to increased surface area, pore structure, and surface functional groups.

The development of new adsorbents and the enhancement of their efficiency were presented in the study by Su et al.[12] They fabricated an adsorbent with over 95% efficiency in removing ciprofloxacin (CIP) within 60 min by embedding MIL-53(Fe) in carbon spheres and employing a hydrothermal coupling and calcination process at 800 °C. Additionally, this adsorbent exhibited high stability across a wide pH range (3.0 to 10.5) and maintained over 85% efficiency even in highly acidic or alkaline conditions.

One of the approaches to enhancing the efficiency of adsorbents is designing them in a porous structure, which increases the contact surface, improves permeability, and accelerates the adsorption process of pollutants. He et al.,[13] using the sol–gel method and dripping technique with konjac glucomannan as a cross-linking agent, developed an aerogel with rapid adsorption kinetics and high capacity for antibiotics such as tetracycline, ofloxacin, and sulfadiazine. The porous structure, low bulk density, and enhanced mechanical and thermal properties strengthened the performance of this composite aerogel, and diverse interaction mechanisms and pH-dependent surface charge further improved its adsorption efficiency.

In the study by Lv et al.,[14] the specific surface area of soil and soil particle size had a significant impact on the adsorption of antibiotics. In this study, soil macroaggregates (with particle sizes of 250–2000 μm) showed the highest adsorption and the lowest desorption. This means that with an increase in the specific surface area in soils with larger particle sizes, the adsorption capacity of antibiotics increases. These results clearly demonstrate that the surface characteristics and structure of the soil can have a significant impact on increasing the adsorption capacity of antibiotics.

Nano hydroxyapatite can be used as a potential adsorbent for removing antibiotics from aqueous environments.[15,16] The nanocrystalline structure and high surface area of nano hydroxyapatite make it a suitable option for adsorbing antibiotic molecules.[17] The surface chemical properties of nano hydroxyapatite, such as phosphate and calcium groups, can interact with antibiotics through mechanisms like hydrogen bonding, ion exchange, and electrostatic attraction.[18,19] Additionally, the ability to adjust the size and specific surface area of hydroxyapatite

nanoparticles allows for improved and optimized adsorption performance.[20] These characteristics make nano hydroxyapatite an efficient adsorbent for water and wastewater treatment and for removing antibiotics, thereby playing a significant role in reducing environmental pollution. However, one of the main challenges in using nanoparticles as adsorbents for antibiotic removal from wastewater is the difficulty in separating nanoparticles from the wastewater after the adsorption process. Due to the small size and high dispersion of nanoparticles, conventional separation methods like filtration and sedimentation are not efficient enough and may lead to the introduction of nanoparticles into the environment, creating new environmental problems. The innovation of this study lies in the use of human hair and bone nanoparticles to produce porous nanocomposite ceramics with high mechanical properties and adsorption capacity. Human hair, as a natural biopolymer, is incorporated into the ceramic matrix, not only improving mechanical properties but also preventing cracking during the initial drying phase. During the calcination phase, the hair disappears, creating suitable porosity in the ceramic. This approach, in addition to enhancing material performance, offers an eco-friendly solution for recycling waste materials such as human hair. Furthermore, the precise control of the hydroxyapatite formation process provides desirable properties for applications like bone tissue engineering and wastewater treatment. Compared to previous studies that focused more on traditional and synthetic materials, this study represents an innovative step towards using natural and sustainable materials with high performance in the production of nanocomposite ceramics.

The main objective of this study is to investigate the antibiotic adsorption process in a semi-industrial method using a fixed bed column. In this context, an experimental design will be developed to study the impact of various factors on the adsorption process, such as contact time, pH, antibiotic concentration, and the amount of adsorbent in the fixed bed. Additionally, the physicochemical properties of the adsorbents, such as surface area, porosity, and chemical composition, will be examined to more accurately assess the performance of the adsorbents in the antibiotic adsorption process. Furthermore, the mechanical and chemical resistance of the adsorbents under different operational conditions will also be evaluated to determine their long-term usability and efficiency in water and wastewater treatment systems.

2. Materials and methods

2.1. Materials

The clay was used as the main base material, sourced from the city of Hamadan, Iran, with its physical and chemical properties

Table 1 Physicochemical characteristics of natural clay

Properties of natural clay						
CEC^a (m_{eq}/100 g)	CE^b (μS)	pH	Ca^{2+} (m_{eq}/100 g)	Mg^{2+} (m_{eq}/100 g)	Na^+ (m_{eq}/100 g)	K^+ (m_{eq}/100 g)
29.37	765	8.2	18.25	8.17	0.58	1.23

^{a} CEC: cation exchange capacity. ^{b} CE: electrical conductivity.

outlined in Table 1. The cow leg used in this study was purchased from a butcher named Mr Reza Naderi in the city of Ben. Cow leg bones were used for the synthesis of hydroxyapatite. First, the meat and fat tissue were removed from the bones, and then, to ensure the removal of all surface and interstitial fat, the bones were boiled for 1 h at 135 °C, repeated three times. After boiling, the bones were fragmented into approximately 6 mm pieces by using a 5 kg hammer. The human hair samples used in this study were collected from Mehdi Akbari, a local barbershop named Javanan Barbershop in the city of Ben; washed at 100 °C for 10 min, and dried at room temperature under a chemical hood. The hair strands were then cut into pieces approximately 10–15 mm in length. Ofloxacin, tetracycline, and sulfadiazine were purchased from Iran Daru Company. Nitric acid, hydrochloric acid, and sodium hydroxide were obtained from Merck. Deionized water was used in all experiments whenever water was required.

Three types of wastewater containing antibiotics ofloxacin (125 mg L^{-1}, pH: 6.52, turbidity: 112 NTU), tetracycline (110 mg L^{-1}, pH: 7, turbidity: 100 NTU), and sulfadiazine (101 mg L^{-1}, pH: 7, turbidity: 92 NTU) were collected from a pharmaceutical company located in Alborz Province, Iran. The required concentrations for the study were obtained by diluting the wastewater samples received from the factory to the desired levels.

2.2. Fabrication of porous nanocomposite ceramics

Bone nanoparticles were produced using a planetary mill at a speed of 650 rpm for 120 min. A total of 250 g of clay was selected as the ceramic base, and varying amounts of bone nanoparticles ranging from 10 to 120 g, as well as human hair in amounts from 10 to 50 g, were added to the clay base. Next, 200 g of water was added to this blend, which was then stirred for 45 minutes with a high-powered mechanical stirrer (Tosan 0901S cordless). The resulting homogeneous mixture was shaped into 4 mm diameter spheres. These spheres were air-dried at room temperature over a period of 4 days. Subsequently, the nano composite ceramics were subjected to calcination at 860 °C for 14 h. To form nano-hydroxyapatite within the ceramic structure, a heating rate of 5 °C min^{-1} was chosen, in accordance with previous studies.[21]

2.3. Experimental design

The wastewater containing antibiotics entered a horizontal column containing the adsorbents and passed over the ceramic adsorbents in a plug flow. In this process, the antibiotics were adsorbed onto the adsorbents. As depicted in Fig. 1a, the column was constructed from plexiglass, measuring 30 mm in diameter and 15 cm in length, with an inlet at the top and an outlet at the bottom. A household evaporative cooler pump was used to circulate the wastewater. In each adsorption experiment, 10 L of antibiotic-contaminated wastewater were introduced into a batch process. The batch adsorption process is schematically shown in Fig. 1b. The study evaluated variables including pH, adsorbent amount, temperature, initial antibiotic
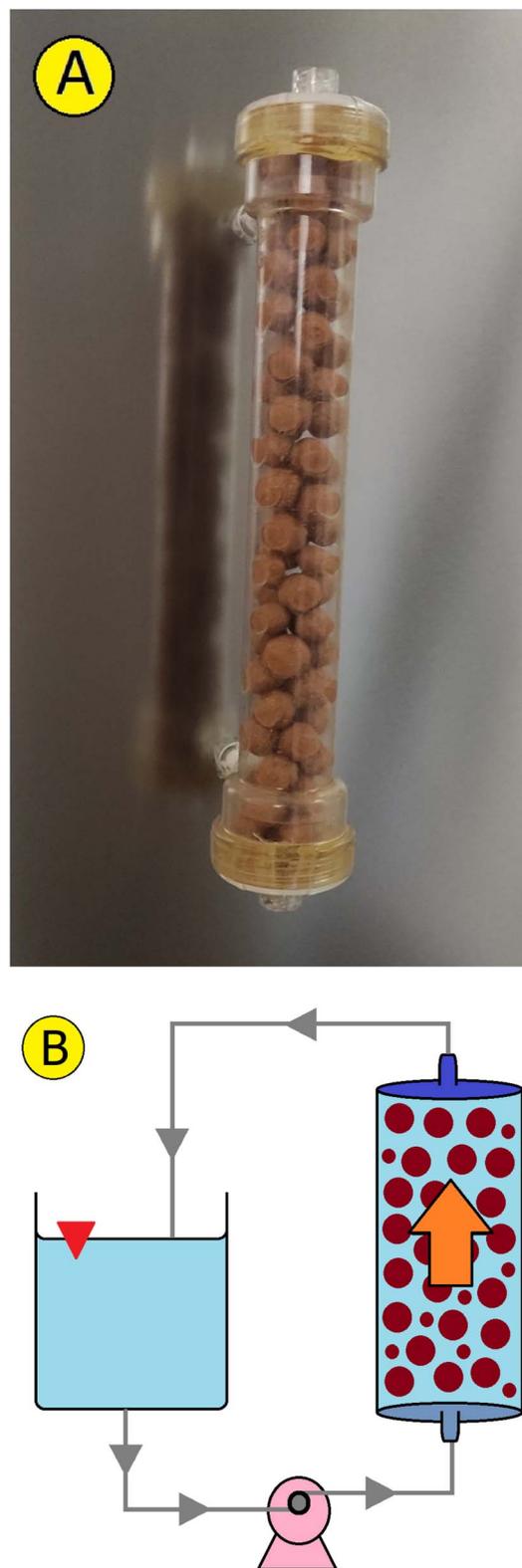

Fig. 1 Nanocomposite ceramics in a fixed-bed column (a) schematic diagram of the adsorption process (b).

concentration, and contact time. A Response Surface Methodology (RSM) experimental design with 50 runs was conducted by Central composite design (CCD). An experimental

Table 2 Levels of independent variables in CCD

Independent variable	Symbol	Levels				
		−2	−1	0	+1	+2
pH	X_1	2	4.32	6	7.68	10
Temperature (°C)	X_2	25	33.69	40	46.31	55
Antibiotic initial concentration (mg L^{-1})	X_3	5	32.53	52.50	72.47	100
Adsorbent mass (g)	X_4	4	10.09	14.50	18.91	25
Retention time (min)	X_5	5	15.14	22.50	29.86	40
Response						
Ofloxacin removal efficiency						R_{OF} (%)
Tetracycline removal efficiency						R_{TE} (%)
Sulfadiazine removal efficiency						R_{SU} (%)

design based on Response Surface Methodology (RSM) was conducted using the Central Composite Design (CCD), resulting in a total of 50 runs. Table 2 shows the minimum and maximum values of the adjustment parameters.

In this study, it is assumed that environmental conditions are constant, the adsorbents behave ideally, there are no interfering compounds, the adsorbent is uniformly distributed, and the data can be fitted to classical adsorption models. The experiments were conducted in triplicate to enhance the accuracy of the results.

2.4. Analytical methods and measurements

Functional groups present in the adsorbent were identified using FT-IR spectroscopy, with spectra obtained from a PerkinElmer C88731 spectrophotometer (Germany). The morphology of the nanocomposite ceramics was provided by a field emission scanning electron microscope (FE-SEM) TE-SCAN. X-ray diffraction (XRD) analysis was conducted with a Philips PW3040 to study the structure of the ceramic adsorbents. Since pore structure plays a key role in antibiotic adsorption, BET surface area and pore size distribution were determined through BET analysis with a Costech Sorptometer 1042. Antibiotic concentrations were measured using UV-Vis spectrophotometry (model UV1900, China), following the standard peak wavelength curves for ofloxacin (289 nm), tetracycline (277 nm), and sulfadiazine (255 nm).[13]

2.5. Evaluation of mechanical and chemical durability

In order to evaluate the mechanical properties of the spherical nanocomposite ceramics, they were positioned between two parallel clamps and exposed to compressive force using a hydraulic press from PerkinElmer, Germany.[22] The pressure required to fracture the spherical adsorbent was recorded as a measure of its mechanical strength. For chemical durability evaluation, the mass loss in the nanocomposite materials following immersion in HNO$_3$ at pH 1 or NaOH at pH 13 solutions for a duration of 10 minutes was measured.[23]

2.6. Formulation of regression model equation

Fifty trials were performed following the experimental plan, with the results for each batch presented in Table S1.† The data obtained from these trials were fitted to a quadratic model. Eqn (1)–(3) were used to predict the interaction effects of key variables on the antibiotic adsorption process. A positive coefficient in these equations indicates a synergistic effect on adsorption efficiency.

$$R_{OF} (\%) = +8.68 + 0.1336X_1 - 0.1218X_2 - 0.5805X_3 + 0.1283X_4 + 0.2139X_5 - 0.1036X_1^2 \quad (1)$$

$$R_{TE} (\%) = +8.79 + 0.1339X_1 - 0.1203X_2 - 0.5685X_3 + 0.1263X_4 + 0.2105X_5 - 0.1123X_1^2 \quad (2)$$

$$R_{SU} (\%) = +8.12 + 0.1016X_1 - 0.1137X_2 - 0.5399X_3 + 0.1193X_4 + 0.1989X_5 - 0.0125X_1^2 \quad (3)$$

3. Results

3.1. Physical strength properties

The incorporation of natural materials and nanoparticles into ceramic composites is widely acknowledged as an efficient approach for improving the mechanical properties and overall performance of ceramics.[24] These combinations can create complex and optimized structures within ceramics, significantly improving their overall functionality. For instance, research has demonstrated that hydroxyapatite nanoparticles, when used as reinforcements in ceramic matrices, enhance both the mechanical and biological properties of ceramics. Similarly, incorporating natural fibers such as hemp and flax into porous ceramics can reduce their weight and increase their strength.[25] The microchannels formed by these fibers improve the permeability and moisture control of the ceramics, indicating the potential of combining natural materials and nanoparticles as an innovative approach to strengthening ceramics.

Studies have shown that adding nano rubber to clay ceramics can reduce fracture stress and increase flexibility.[22] Moreover, the addition of hydroxyapatite nanoparticles to

sponge-like ceramics with flat geometric shapes has been shown to enhance their resistance to fracture pressures. This indicates that nanoparticles are instrumental in improving the mechanical properties and in effectively managing internal stresses within the ceramics.

According to the results presented in Fig. 2a, the structural durability of the ceramic samples composed of 450 g clay, 50 g human hair, and 100 g cow bone powder (optimal ratio) was significantly elevated at the highest level. These ceramics exhibited a fracture stress that was 3.6 bar higher compared to those reinforced with nano rubber or nano hydroxyapatite. This improvement in mechanical strength is attributed to the synergistic effects of bone powder's reinforcing properties and the formation of microchannels created by the human hair. These microchannels facilitate moisture removal during drying and contribute to stress absorption and distribution, thereby significantly boosting the overall mechanical resistance of the ceramics.

3.2. Chemical resistance

Chemical resistance in ceramics refers to their ability to withstand degradation and decomposition in various chemical environments without losing their core mechanical and physical properties.[26] Oxide-based ceramics such as alumina, zirconia, and silica exhibit high chemical resistance due to their strong atomic bonds, making them highly resilient in acidic and alkaline environments.[27] The physical structure of ceramics also plays a crucial role; dense ceramics typically offer better chemical resistance compared to porous ones. The introduction of nanoparticles in nanocomposites can further enhance this resistance.[28] Additionally, factors like temperature and pH significantly impact the chemical resistance of ceramics; they perform better in low temperatures and neutral pH but can show reduced resistance under high temperatures or extreme pH conditions.[29]

A stable and porous nanocomposite ceramic was prepared with an optimal ratio of components. As shown in Fig. 2b, nanocomposite ceramic exhibited significant resistance when exposed to NaOH at pH = 13 and HNO$_3$ at pH = 1. At a retention time of 30 h, the weight loss in these solutions was under 0.19% and 0.27%, respectively. Even after 280 h, the reduction in weight stayed minimal, with values below 1.07% and 1.92% for each case. These findings indicate that nanocomposite ceramics containing hydroxyapatite nanoparticles exhibit greater overall resistance in alkaline solutions compared to acidic ones.

3.3. Analysis of nanocomposite ceramic properties

The FTIR spectrum shown in Fig. 2c of the ceramic nanocomposite confirms the presence of HA through these characteristic bands. According to Fig. 2c, the hydroxyl group (–OH) in hydroxyapatite typically appears as a strong band in the range of 3000–3570 cm^{-1}.[30] In the FTIR spectrum of the hydroxyapatite-containing ceramic nanocomposite, this band is observed at 3573 cm^{-1}, indicating the presence of OH stretching vibrations and confirming the presence of hydroxyapatite. The phosphate
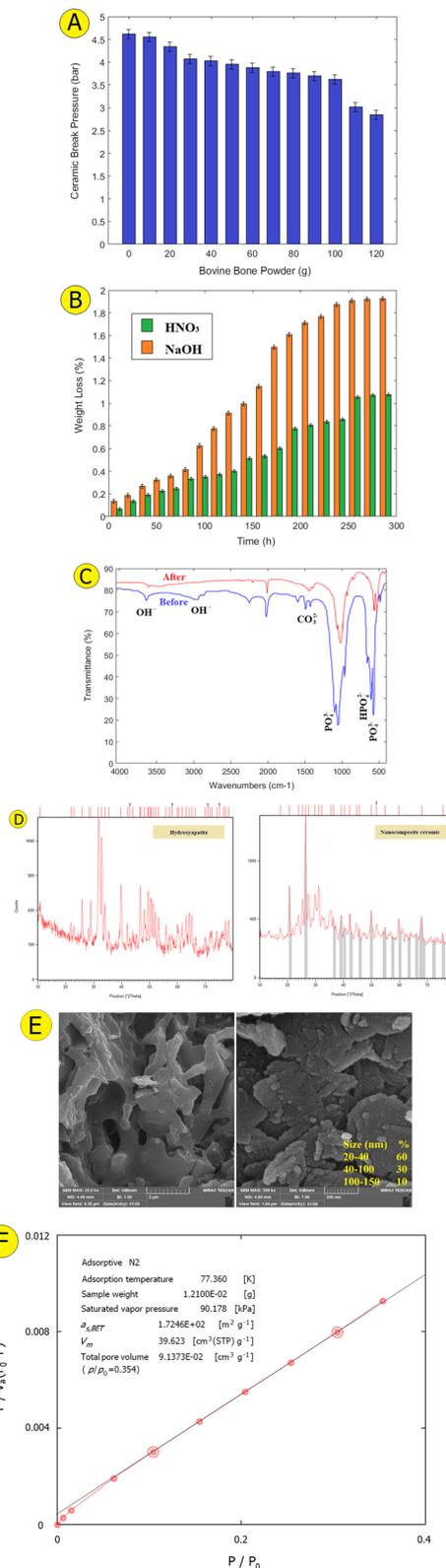

Fig. 2 Effect of bone powder mass (hydroxyapatite) on the mechanical strength of the nanocomposite ceramic adsorbent (a), chemical resistance of the nanocomposite ceramic in acid (pH 1) and base (pH 13) solutions (b), FT-IR spectra (c), X-ray diffraction patterns of hydroxyapatite and nanocomposite ceramics (d), FE-SEM image (e), BET analysis (f).

group $(PO_4)^{3-}$ generates stretching bands in the 900–1100 cm^{-1} region and bending bands in the 400–700 cm^{-1} range, with a prominent band at 1045 cm^{-1} attributed to the stretching vibrations of phosphate.[31] Additionally, bands associated with carbonate groups CO_3^{2-} are observed in the 1400–1600 cm^{-1} range, and hydrogen phosphate groups HPO_4^{2-} appear in the 2800–3000 cm^{-1} range.[32] These bands may indicate substitution or impurities within the hydroxyapatite structure.

Fig. 2d shows the X-ray diffraction (XRD) spectrum of hydroxyapatite extracted from cow bone, which aligns closely with the JCPDS reference hydroxyapatite card (file no. 96-900-1234). The XRD spectrum of the prepared sample exhibits all the characteristic peaks of standard hydroxyapatite clearly and distinctly.[33] The XRD analysis revealed that kaolinite ($Al_2Si_2O_5(OH)_4$) is the primary mineral component in the clay ceramics, with additional peaks indicating the presence of quartz (SiO_2), microcline ($KAlSi_3O_8$), and halloysite ($KAl_2(AlSi_3)O_{10}(OH)_2$). These minerals, particularly kaolinite, contribute to the ceramics' thermal stability and mechanical strength.

In order to examine the morphology of hydroxyapatite nanoparticles and assess the porous structure of the nanocomposite ceramics, Field Emission Scanning Electron Microscopy (FE-SEM) was employed, as illustrated in Fig. 2e. The FE-SEM images showed that hydroxyapatite nanoparticles, averaging around 60 nm in size, were located within the porous regions of the clay ceramics. These nanoparticles were uniformly distributed across the ceramic matrix, indicating a robust interaction between the hydroxyapatite and ceramic components. Furthermore, as depicted in Fig. 2f, a specific surface area measuring 17 132 m^2 g^{-1} and a total pore volume reaching 913.73 cm^3 g^{-1}.

3.4. Hydraulic conductivity of nanocomposite ceramics

The water permeability of ceramics was evaluated using a novel method involving the passage of water over the ceramic surface. In this procedure, a 3 mm open-ended hole was drilled from the surface of the ceramic to the center of a ceramic nanocomposite sphere using an electric drill.[25] The drilled sphere was then
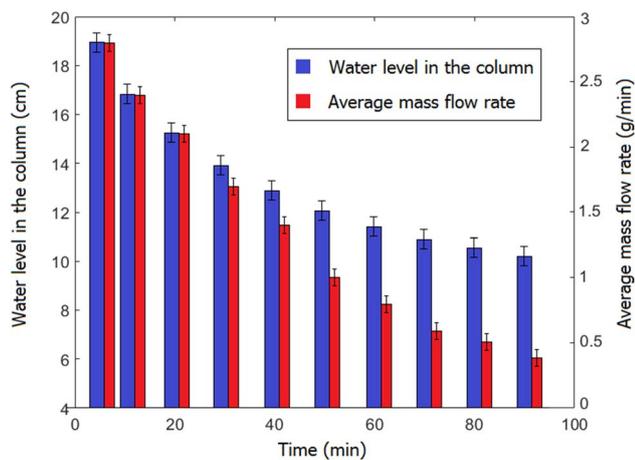

Fig. 3 Correlation between the water level in the column and the average mass flow rate through the nanocomposite ceramic.
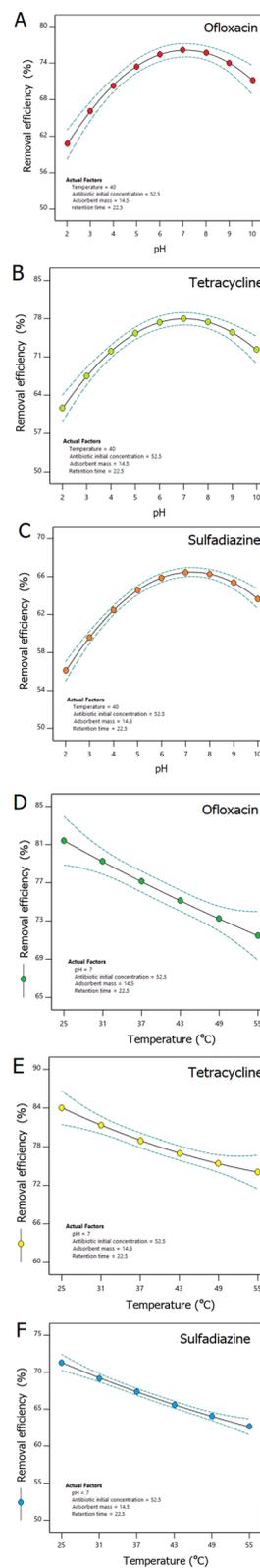

Fig. 4 Effect of pH (a–c) and temperature (d–f) on the removal efficiency of antibiotics.

installed at the end of a vertical glass tube, measuring 4 cm in diameter and 20 cm in length.[21] The tube was filled with water, which infiltrated the ceramic nanocomposite due to its porous structure and drained through the drilled opening. Based on Fig. 3, which illustrates the acceptable permeability of the ceramic at various water pressures, the use of human hair to create porosity was confirmed.

3.5. Process of adsorption

3.5.1. pH. The adsorption of antibiotics is strongly affected by the pH of the environment. Under acidic conditions, adsorbents absorb protons and acquire a positive surface charge, enhancing the uptake of negatively charged antibiotics due to electrostatic attraction. Conversely, at high pH levels, adsorbents lose protons, resulting in a negative surface charge, thereby favoring the uptake of positively charged antibiotics while reducing the absorption of negatively charged ones due to electrostatic repulsion.[34] In modified phosphoric acid biochar, the absorption of sulfamethoxazole decreases at higher pH levels due to electrostatic repulsion.[11] The optimal pH for the absorption of tetracycline by graphene oxide and activated carbon is around 6, where tetracycline exists in its zwitterionic form, reducing electrostatic repulsion and increasing surface absorption.[35] Moreover, in this pH range, the absorption of tetracycline by phosphoric acid-modified biochar and nanoparticles (ZnBC-600 and SBC-600) is also optimal due to stronger interactions between tetracycline's zwitterionic form and the adsorbent surface.[11] Hydrogen bonding is also enhanced in acidic environments, further facilitating absorption, while van der Waals interactions are less affected by pH variations but can indirectly be influenced by changes in the ionic form and molecular structure of antibiotics.[12]

According to Fig. 4a–c, pH 7 acts as an equilibrium point where the adsorption capacity of ceramic adsorbents containing hydroxyapatite nanoparticles is improved for various types of commonly found antibiotics in wastewater, ensuring efficient removal. Hydroxyapatite, as a calcium phosphate mineral, exhibits good stability within a neutral to slightly basic pH range. At pH 7, hydroxyapatite nanoparticles are less prone to dissolution or chemical alteration, ensuring their integrity during the adsorption process. At pH 7, hydroxyapatite nanoparticles typically carry a net negative surface charge due to deprotonation of surface hydroxyl groups and phosphate ions. The presence of a negative surface charge can improve the adsorption of positively charged antibiotics such as ofloxacin and tetracycline. This is due to the electrostatic attraction between the negatively charged surface of the adsorbent and the positively charged antibiotic molecules, which boosts the adsorption efficiency. Considering the solubility of antibiotics, ofloxacin, tetracycline, and sulfadiazine are relatively stable and soluble within a neutral pH range. Therefore, at pH 7, these antibiotics are present in their molecular forms, allowing for effective interaction and adsorption onto the hydroxyapatite-containing ceramic adsorbents. pH 7 may provide an optimal environment for the extensive removal of antibiotics, including ofloxacin, tetracycline, and sulfadiazine, as it balances the
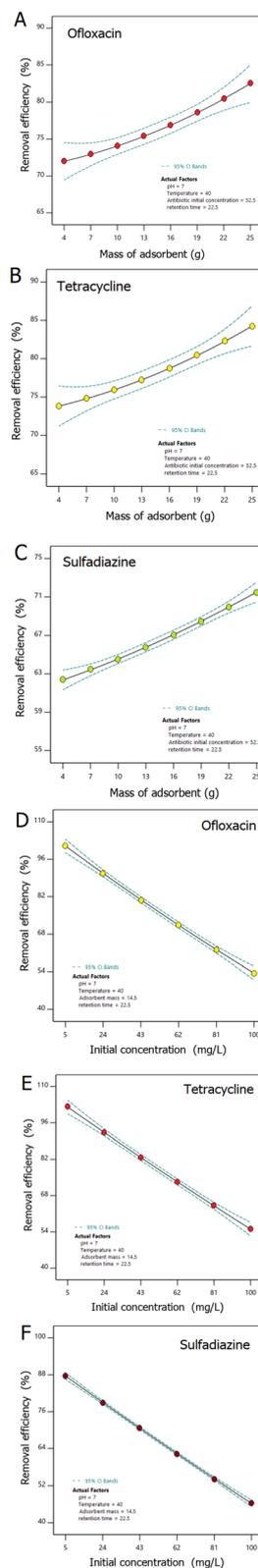

Fig. 5 Impact of adsorbent mass (a–c) and initial antibiotic concentration (d–f) on removal efficiency.

chemical stability of the adsorbent, the solubility of antibiotics, and the surface charge characteristics conducive to adsorption, ensuring improved efficiency of wastewater treatment.

3.5.2. Temperature. In the process of adsorbing antibiotics from wastewater onto adsorbents, temperature plays a crucial role in determining the efficiency of the adsorption process.[36] Generally, an increase in temperature leads to an increase in the molecular motion and kinetic energy of the antibiotics, which can result in more effective collisions between the antibiotic molecules and the adsorbent surface.[37] This enhanced collision rate often leads to improved adsorption at higher temperatures, particularly when the adsorption process is endothermic. However, in some cases, it is observed that adsorption is more efficient at lower temperatures.[38] According to Fig. 4d–f, the adsorption efficiency of antibiotics decreases as the temperature rises from 25 °C to 55 °C. This phenomenon may be attributed to the exothermic nature of the adsorption process, where the system tends to release heat, and as the temperature rises, the propensity for adsorption decreases. Additionally, increasing the temperature can lead to undesirable alterations in the surface architecture of the material or decrease the density of functional sites available for uptake, thereby reducing the overall adsorption efficiency. At higher temperatures, the solubility of the antibiotic molecules in the liquid phase may also increase, and desorption processes from the adsorbent surface can become more pronounced. Khanday *et al.*[39] synthesized activated carbon from chitosan using single-step H_3PO_4 activation and investigated the adsorption of amoxicillin and doxycycline. Their results showed that increasing the temperature (30–50 °C) enhanced the adsorption capacity, indicating an endothermic process. In contrast, in the present study, adsorption decreased with increasing temperature, which may be attributed to differences in the nature of the adsorbent and adsorption mechanism. Hu *et al.*[40] investigated the effect of temperature on the antibiotic adsorption process using $Fe_3O_4@mSiO_2/NH_2$. Their results showed that the adsorption capacity of ciprofloxacin and doxycycline decreased with an increase in temperature, indicating a heat-releasing adsorption process, while the removal efficiency of norfloxacin increased, suggesting the endothermic nature of the process. These results are in contrast to our study, where adsorption efficiency continuously decreased with increasing temperature, likely due to the exothermic nature of the process. This discrepancy may arise from differences in the surface characteristics of the adsorbent, antibiotic interactions, or the effect of temperature on the adsorption–desorption equilibrium.

3.5.3. Antibiotic concentration and adsorbent mass. The adsorbent mass has a direct impact on the availability of active sites for antibiotic adsorption, and as it increases, the number of active sites available for the adsorption process also rises. At pH 7, temperature 40 °C, initial antibiotic concentration of 52.5 mg L^{-1}, and a retention time of 22.5 min, Fig. 5a–c shows the removal efficiency at different adsorbent masses (4–25 g). According to the experimental results, removal efficiency of antibiotics increased with increasing adsorbent mass. Increasing the adsorbent dose typically enhances the contact surface area between the antibiotics and the adsorbent, improving the adsorption of antibiotics onto the adsorbent surface. This can lead to faster and more effective removal of

antibiotics from the aqueous solution. However, at very high adsorbent doses, a decrease in adsorption efficiency may be observed due to the saturation of the adsorbent surface and the reduction in adsorption capacity. Therefore, determining the optimal adsorbent dose is essential to achieve maximum removal efficiency of antibiotics with minimal material usage. Fig. 5d–f illustrates that removal efficiency decreased with increasing initial antibiotic concentration in the wastewater. The synergistic effect of these two parameters (adsorbent mass and initial antibiotic concentration) is depicted in Fig. 6a–c.
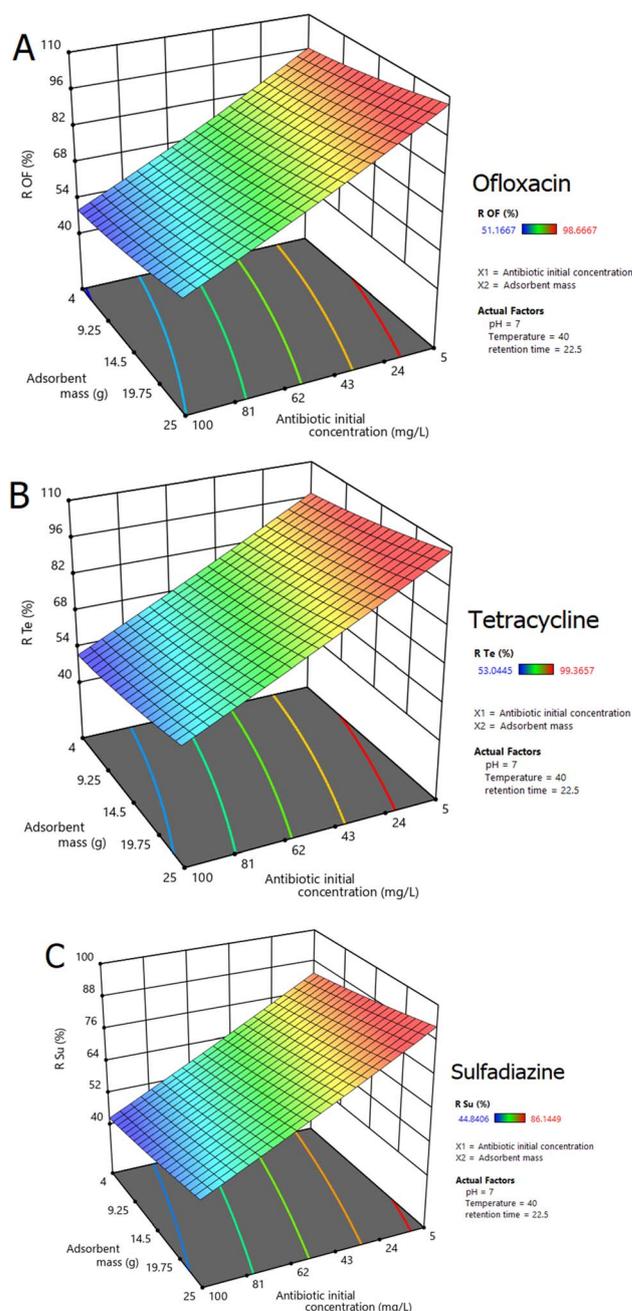

Fig. 6 Synergistic effect of adsorbent mass and initial antibiotic concentration on removal efficiency of ofloxacin (a), tetracycline (b) and sulfadiazine (c).

Increasing the initial concentration of antibiotics in the aqueous solution can lead to a higher initial adsorption rate and enhance the adsorbent's ability to remove antibiotics. This is because a greater concentration gradient exists between the aqueous phase and the adsorbent surface, providing a stronger driving force for the transfer of antibiotic molecules to the adsorbent surface. However, at very high concentrations, the adsorbent's capacity may quickly become saturated, resulting in decreased adsorption efficiency since all the active sites on the adsorbent become occupied and cannot accommodate more molecules.

3.5.4. Time and kinetics. As illustrated in Fig. 7a, the uptake of antibiotics from water by the adsorbent occurs remarkably quickly within the initial 30 min, which is attributed to the high availability of reactive sites on the nanocomposite ceramic adsorbent surface. The equilibrium adsorption time for antibiotics in pH 7, temperature 25 °C, initial concentration of 52.5 mg L^{-1}, and 14.5 g of adsorbent, was monitored over a period of 5 to 80 min. Between 30 and 40 min, the adsorption rate begins to decrease, and from 40 to 60 min, the rate slows even further. The shift in the slope of the adsorption curve indicates that equilibrium is reached after 80 min.

According to Fig. 7b–d, under the same constant conditions (pH, temperature, and adsorbent mass), increasing the initial concentration of antibiotics did not alter the kinetic behavior of adsorption. In other words, the adsorption rate exhibited the same slope up to 40 minutes for all concentrations. However, the adsorption efficiency decreased because the available active sites for the antibiotics became limited. Additionally, with higher initial concentrations of antibiotics, there is a greater likelihood of antibiotic aggregation on the adsorbent surface, leading to blockage of the porous adsorbent's microchannels. This phenomenon is another critical factor contributing to the reduction in adsorption efficiency.

The adsorption kinetics were evaluated using three different models: the pseudo-first-order, pseudo-second-order, and intraparticle diffusion models. The corresponding equations for these kinetic models are as follows:[41]

$$\log(q_e - q_t) = \log q_e - \left(\frac{k_1}{2.303}\right)t \quad (6)$$

$$\frac{1}{q_e - q_t} = \frac{1}{q_e} + k_2 t \quad (7)$$

$$q_e = k_3 t^{0.5} + C \quad (8)$$

In these equations, q_e and q_t (mg g^{-1}) denote the adsorption capacities at equilibrium and at a given time t (min^{-1}) respectively. The rate constants k_1 (min^{-1}) for pseudo-first-order, k_2 (mg (g min)$^{-1}$) for pseudo-second-order and, k_3 (mg g^{-1} min$^{-0.5}$) correspond to intraparticle diffusion models.

Table 3 presents the results of the data fitting based on the kinetic models. The conformity with the pseudo-first-order model ($R^2 > 0.98$) indicates that the adsorption process in the initial stages depends on the amount of adsorbed material and is controlled by the surface adsorption rate. In the pseudo-first-
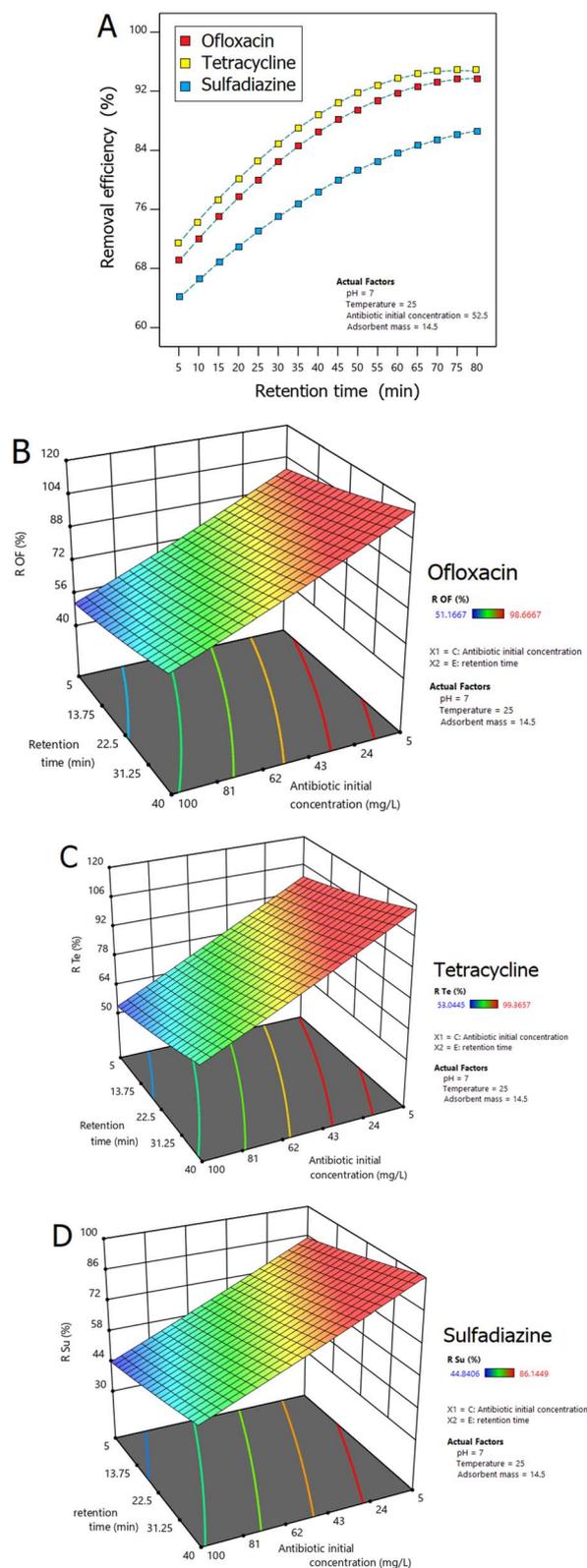
Fig. 7 Effect of retention time on removal efficiency of antibiotics (a), synergistic effect of retention time and initial antibiotic concentration on removal efficiency of ofloxacin (b), tetracycline (c) and sulfadiazine (d).

order model, the adsorption rate is higher at the beginning of the process because more active surface sites are available for adsorption, which gradually decreases over time. Furthermore, high conformity with the intraparticle diffusion model ($R^2 >$ 0.99) suggests that the adsorption process is limited by the diffusion of the material within the adsorbent particles, especially in the later stages when the adsorbate is transferred to internal active sites. In the intraparticle diffusion model, the movement of adsorbate molecules within the adsorbent's microchannels determines the rate of the process in the later stages, as access to active surface sites decreases and the molecules must migrate within the adsorbent particles.

4. Optimizing process and modeling techniques

The optimal conditions were selected using Design Expert software through a desirability analysis approach. In this method, the software assesses the effects of various parameters (such as pH, temperature, initial antibiotic concentration, adsorbent amount, and contact time) by adjusting them within a defined range, creating multiple combinations of experimental conditions, and calculating the adsorption efficiency for each combination. In the next step, the software assigns a desirability score to each combination. This score is a numerical value between 0 and 1, representing how close each combination is to the optimal conditions; a score of 1 indicates the highest alignment with the optimization goal. The combination with the highest desirability is then proposed as the optimal condition. As shown in Fig. 9a, in this study, the selected optimal combination had a desirability of 0.828 and included a pH of 7.2, 25 g of ceramic nanocomposite, a temperature of 25 °C, an initial concentration of 51.42 mg L^{-1}, and a contact time of 40 min.

4.1. Thermodynamic analysis

The thermodynamic characteristics of the antibiotic adsorption process from industrial wastewater were investigated, and the thermodynamic parameters including Gibbs free energy (ΔG), enthalpy (ΔH), and entropy (ΔS) were calculated.[42] These parameters evaluate the energy characteristics and stability of the adsorption process by determining the relationship between the concentration of the adsorbed substance and temperature. They are used to describe the spontaneity, exothermic or endothermic nature, and order or disorder of the adsorption process.

$$\Delta G = -RT \ln K_d \tag{9}$$

$$K_d = \lim_{time \to \infty} \frac{C_{es}}{C_{el}} \tag{10}$$

$$K_d = \frac{C_{es}}{C_{el}} = \frac{C_0 - C_e}{C_0} \tag{11}$$

$$\ln K_d = \frac{\Delta S}{R} - \frac{\Delta H}{RT} \tag{12}$$

In this context, C_{el} and C_{es} (mg L^{-1}) refer to the equilibrium concentrations in the liquid and solid phases, respectively. The gas constant R is valued at 8.314 J mol^{-1} K^{-1} while T represents the absolute temperature in Kelvin (K). The term K_d denotes the distribution coefficient. As indicated in Table 4, this research focused on analyzing the thermodynamic parameters related to the adsorption of the antibiotics ofloxacin, tetracycline, and sulfadiazine onto a nanocomposite ceramic adsorbent. The analysis showed that the ΔH for all three antibiotics was positive, indicating an endothermic process. In other words, energy in the form of heat is required for adsorption to occur. The ΔH values for ofloxacin, tetracycline, and sulfadiazine were 12.33, 15.67, and 4 kJ mol^{-1} respectively. On the other hand, the ΔS for all three antibiotics was negative, indicating a decrease in the system's disorder during the adsorption process. The ΔS values for ofloxacin, tetracycline, and sulfadiazine were -0.138, -0.182, and -0.036 kJ mol^{-1}, respectively. The ΔG was negative at various temperatures, indicating the spontaneity of the adsorption process. However, the negative ΔG values decreased with increasing temperature, suggesting a reduction in the spontaneity of the adsorption process. For instance, for

Table 3 Overview of adsorption data analyzed with multiple kinetic models

| Wastewater sample | q_{max} (mg g^{-1}) | Pseudo first-order model | | | Pseudo second-order model | | | Intra particle diffusion model | | |
		q_e (mg g^{-1})	K_1 (min^{-1})	R^2	q_e (mg g^{-1})	K_2 (mg g^{-1} min^{-1})	R^2	K_3 (mg g^{-1} min$^{-0.5}$)	C	R^2
Ofloxacin	149.76	51.04	0.0382	0.982	461.66	0.0022	0.880	4.23	58.97	0.996
Tetracycline	151.69	46.09	0.0382	0.978	526.32	0.0025	0.828	6.38	101.31	0.988
Sulfadiazine	137.68	43.40	0.0332	0.988	99.01	0.0019	0.914	6.05	88.14	0.995

Table 4 Thermodynamic analysis of antibiotic adsorption on nano-composite ceramic

| Wastewater sample | K_d | | | ΔH (kJ mol^{-1}) | ΔS (kJ mol^{-1}) | ΔG (kJ mol^{-1}) | | | R^2 |
	25 °C	40 °C	55 °C			25 °C	40 °C	55 °C	
Ofloxacin	49	12.33	7.35	-50.275	-0.138	-9.65	-6.54	-5.44	0.935
Tetracycline	99	15.67	9.01	-64.960	-0.182	-11.39	-7.16	-5.99	0.922
Sulfadiazine	5.67	4	3.26	-14.82	-0.036	-4.30	-3.61	-3.22	0.970

ofloxacin, ΔG at 25 °C, 40 °C, and 55 °C were −9.65, −6.54, and −5.44 kJ mol^{-1}, respectively. These results indicated that despite the endothermic nature of the adsorption process, the decrease in system disorder and its negative impact on ΔG cause the adsorption efficiency to decrease with increasing temperature. Therefore, the adsorption of antibiotics onto the nano-composite ceramic adsorbent is more optimal and effective at lower temperatures.

4.2. Models of adsorption in fixed bed column

The adsorption equilibrium model in fixed bed column provides a critical framework for describing how substances transfer from the aqueous phase to a solid adsorbent at a constant temperature. This concept is vital for understanding the equilibrium state in adsorption processes. Various isotherm models are employed to interpret the equilibrium data, including the Langmuir model, which assumes monolayer adsorption on a uniform surface; the Freundlich model, which addresses multilayer adsorption on diverse surfaces; and the Dubinin–Radushkevich (D–R) model, which aids in identifying the adsorption mechanism and energy properties of the adsorbent. As shown in Table 5, both the Langmuir and Freundlich models yielded high coefficients of determination ($R^2 > 0.99$), indicating an excellent fit for the equilibrium adsorption data. This suggests that both models effectively capture the adsorption behavior of antibiotics on the

nanocomposite ceramic adsorbent. The Langmuir model is based on the premise of monolayer adsorption on a uniform surface, while the Freundlich model accommodates multilayer adsorption on a non-uniform surface. The strong correlation with both models implies that the adsorption system exhibits characteristics of both monolayer and multilayer adsorption, as well as surface heterogeneity of the adsorbent.

4.3. Mechanisms of adsorption

The components of this nanocomposite adsorbent are natural clay and hydroxyapatite, which is added as an additive.[43] This combination imparts unique surface and structural properties to the adsorbent, enhancing its ability to adsorb antibiotics.[11] Montmorillonite, classified as a clay mineral, has a consistent electrical charge on its exterior that is neutralized through the presence of swapable cations.[44] These cations can be replaced by antibiotic molecules during the adsorption process, leading to their attachment to the adsorbent surface. The FTIR spectrum suggests that an ion exchange takes place between the antibiotic molecules and reactive sites, such as hydroxyl (–OH) and phosphate $(PO_4)^{-3}$,[45] found in hydroxyapatite (Fig. 8).

The adsorption of antibiotic molecules onto the adsorbent surface is due to the presence of weak attractive forces (van der Waals) between the adsorbent surface and the molecules. In physical adsorption, the antibiotic molecules are attached to the adsorbent surface due to weak intermolecular forces.[38] This

Table 5 Isotherm parameters for the adsorption of antibiotics onto nano-composite ceramic

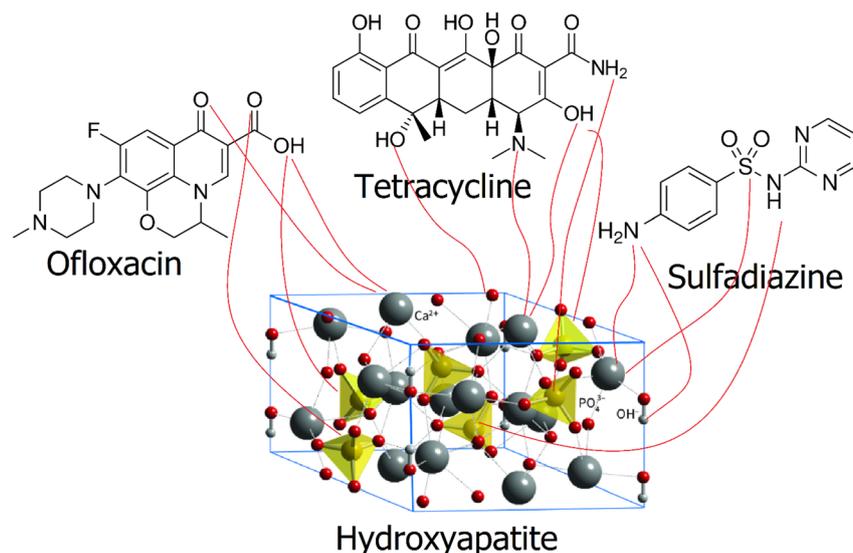| Wastewater sample	Langmuir			Freundlich			Dubinin–Radushkevich			
	q_{max} (mg g^{-1})	b (L mg^{-1})	R^2	K_F (mg g^{-1})	n	R^2	q_{DR} (m mol g^{-1})	β_{DR} (mol^2 J^{-2})	E (kJ mol^{-1})	R^2
Ofloxacin	19.92	2.202	0.994	7.488	2.315	0.996	115.446	0.000001	0.707	0.843
Tetracycline	22.47	1.926	0.995	8.946	2.059	0.995	116.478	0.0000005	1.000	0.857
Sulfadiazine	18.87	2.345	0.993	6.896	2.443	0.996	118.746	0.000002	0.500	0.878

Fig. 8 Schematic of the mechanism of binding of antibiotics to functional groups on the surface of hydroxyapatite.

type of adsorption is reversible and usually more effective at lower temperatures. In the process of chemical surface adsorption, either strong or weak interactions are established within the antibiotic molecules and the functional sites attached to the adsorbent's surface.

These bonds are stronger than physical forces, resulting in a more robust attachment of the antibiotics to the adsorbent surface. This type of adsorption is typically irreversible and more effective under specific conditions, such as pH and temperature. Due to its ordered crystalline framework and high ion exchange potential, hydroxyapatite is capable of absorbing calcium and phosphate ions. These properties enhance hydroxyapatite's ability to effectively adsorb antibiotic molecules. Hydroxyapatite, due to its biological compatibility and environmental degradability, is a suitable material for environmental applications. The Freundlich isotherm model highlights the importance of multilayer adsorption and the heterogeneous nature of the adsorbent surface in the
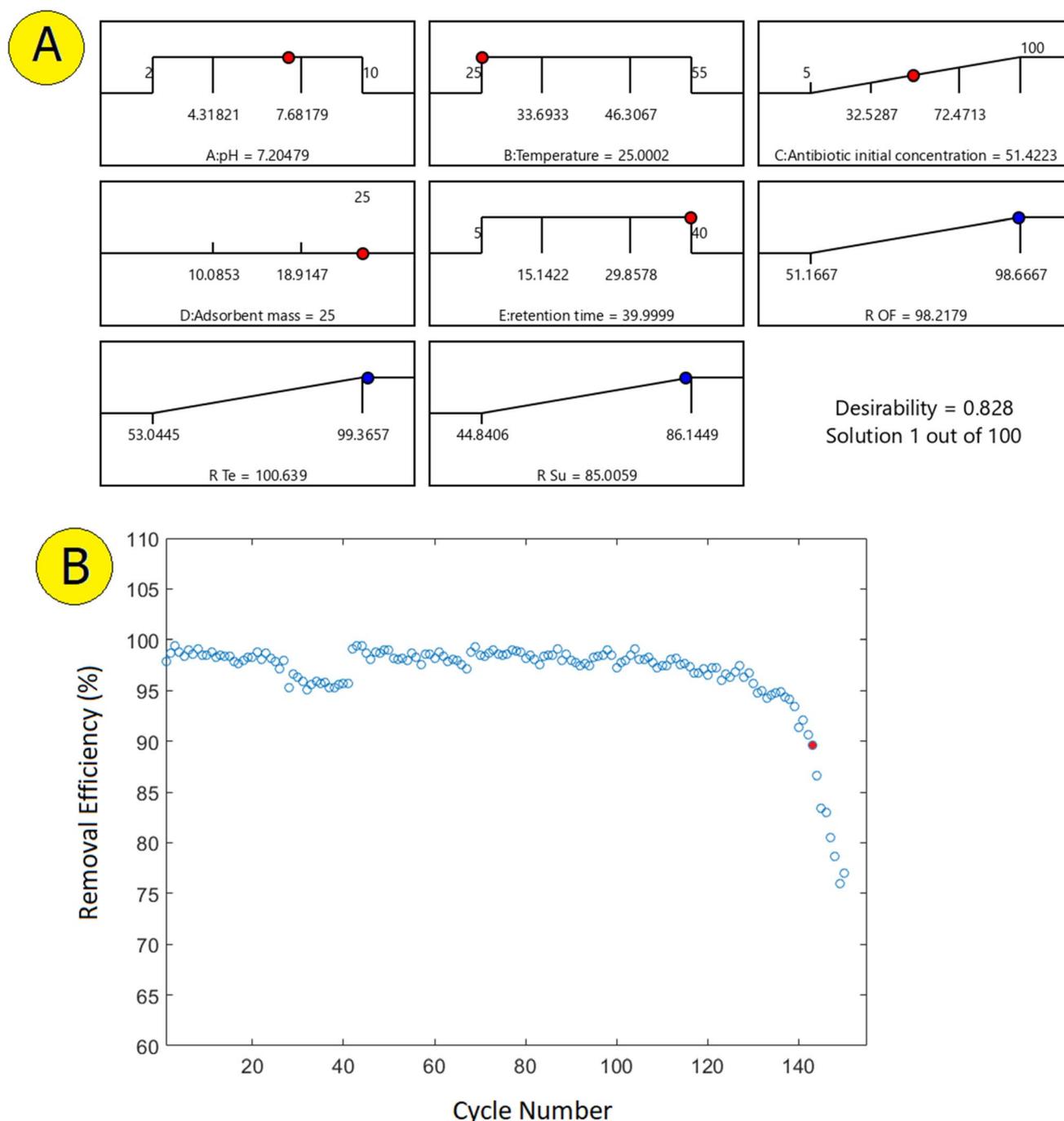

Fig. 9 Desirability ramp for the numerical optimization of affecting factors on the process response (a). Antibiotics removal efficiency after successive regenerations of the adsorbent (b).

adsorption process. This model implies that the adsorption sites on the adsorbent have varying energy levels, facilitating multilayer adsorption. Collectively, these mechanisms enhance the effective adsorption of ofloxacin, tetracycline, and sulfadiazine by the nanocomposite ceramic adsorbent. These findings suggest that this adsorbent could serve as an efficient solution for treating water contaminated with antibiotics.

5. Regeneration of the adsorbent

Regeneration of the adsorbent in adsorption processes, especially for practical applications in wastewater treatment, is a crucial aspect.[19,46] The ability to effectively regenerate the adsorbent ensures its long-term usability and cost-effectiveness. In this study, the performance of the adsorbent in removing antibiotics was tested over 150 cycles, demonstrating its stability and durability. The regeneration process involved immersing the adsorbent in 37% hydrochloric acid and then rinsing it with water to remove any remaining acid. This method effectively restored the adsorbent's capacity, maintaining a removal efficiency of over 90% up to the 142nd cycle (Fig. 9b). The successful regeneration of the adsorbent highlights its potential for repeated use in treating antibiotic-contaminated water, reducing the need for frequent replacement, and minimizing operational costs. The ability to regenerate the adsorbent while maintaining high efficiency underscores its practicality for large-scale and long-term applications in environmental remediation.

6. Future research

Although the current study provides valuable insights into the synthesis and application of ceramic nanocomposites for antibiotic removal, several areas can be explored in future research. First, further studies should focus on optimizing the synthesis process to enhance the efficiency and selectivity of the nanocomposites for different types of antibiotics and pollutants. Additionally, it would be beneficial to explore the long-term performance and stability of these nanocomposites in real-world wastewater treatment applications, including their interactions with various contaminants present in complex water matrices.

Another important area of future research involves investigating the recycling and regeneration processes of these nanocomposites to determine their feasibility in large-scale applications. More efficient methods of regenerating the adsorbent without compromising its performance should be explored. Moreover, the environmental impact of using such nanocomposites, including the life cycle analysis (LCA), should be considered to assess their sustainability and economic viability.

Finally, incorporating other naturally occurring materials, such as plant-based biopolymers or marine-sourced substances, could further enhance the performance and sustainability of the nanocomposites. Investigating the synergistic effects of multi-component nanocomposites could lead to even more efficient solutions for environmental remediation.

7. Conclusion

The synthesis of the ceramic nanocomposite successfully integrated natural clay and hydroxyapatite, yielding an adsorbent with distinct surface and structural properties. The incorporation of hydroxyapatite, characterized by its well-ordered crystalline form and substantial ion-exchange capacity, played a pivotal role in enhancing the adsorption performance. Its biocompatibility and degradability further underscore its potential for environmental applications, particularly in the treatment of antibiotic-contaminated wastewater.

The developed nanocomposite demonstrated a high density of functional groups, contributing to its complex and effective adsorption mechanisms. It exhibited strong adsorption capabilities, efficiently removing antibiotics such as ofloxacin, tetracycline, and sulfadiazine from aqueous solutions. The mechanical robustness of the material was evident, withstanding pressures up to 3.6 bar, ensuring structural integrity under practical operating conditions. Moreover, the adsorbent displayed exceptional chemical stability, with negligible weight loss in both acidic and alkaline environments (0.19% in NaOH and 0.27% in HNO_3 after 30 hours), making it a durable candidate for long-term use.

The thermodynamic analysis provided deeper insights into the adsorption process. The positive enthalpy values (ΔH = 12.33, 15.67, and 4 kJ mol^{-1}) confirmed the endothermic nature of the adsorption, suggesting that increased temperature enhances adsorption efficiency. The negative Gibbs free energy values (ΔG) at various temperatures indicated the spontaneity and feasibility of the process, emphasizing the strong affinity between the nanocomposite and antibiotic molecules. The adsorption mechanisms were further elucidated through FTIR analysis, revealing contributions from ion exchange, physical adsorption via van der Waals forces, and chemical adsorption through covalent or ionic interactions. The adsorption behavior conformed to both Langmuir and Freundlich isotherm models, indicating the presence of both monolayer and multilayer adsorption on a heterogeneous surface, which enhances the adsorbent's versatility in real wastewater applications.

One of the most remarkable attributes of this nanocomposite is its outstanding regenerability. The adsorbent maintained over 90% removal efficiency up to the 142nd regeneration cycle, which involved immersion in 37% hydrochloric acid followed by water rinsing. This high level of reusability significantly reduces operational costs and material waste, making it a viable solution for large-scale wastewater treatment. The long-term stability and efficiency of the adsorbent highlight its potential for industrial applications, particularly in pharmaceutical wastewater treatment plants where persistent antibiotic contamination is a critical concern.

Beyond its adsorption performance, the development of this nanocomposite aligns with the principles of environmental sustainability. The utilization of clay, bone-derived hydroxyapatite, and human hair-derived biopolymers contributes to a circular economy by repurposing natural and recycled materials, minimizing the reliance on synthetic raw materials. This

not only reduces the environmental footprint but also offers a cost-effective and eco-friendly alternative to conventional adsorbents. Moreover, the non-toxic composition of these nanocomposites ensures that no secondary pollution is introduced into treated water, making them a safer alternative for large-scale environmental remediation.

The broader implications of this study extend to improving global wastewater treatment strategies. As antibiotic pollution continues to rise due to excessive pharmaceutical discharge, the need for efficient, sustainable, and regenerable adsorbents is critical. The findings from this study provide a foundation for further optimization of bio-based nanocomposites, paving the way for the development of more advanced materials tailored for targeted pollutant removal. Future research could explore the scalability of this technology, its effectiveness in real wastewater matrices, and its performance in removing other emerging contaminants such as pesticides and personal care products.

In this study presents a ceramic nanocomposite with exceptional adsorption efficiency, high reusability, and environmental sustainability. Its robust mechanical and chemical stability, along with its cost-effective regeneration process, makes it a promising candidate for large-scale wastewater treatment. By integrating biodegradability, recyclability, and high adsorption capacity, this nanocomposite not only addresses pressing environmental challenges but also contributes to the advancement of sustainable water purification technologies.

Ethical statement

The cow leg used in this study was purchased from a butcher named Mr Reza Naderi in the city of Ben. The human hair samples used in this study were collected from Mehdi Akbari, a local barbershop named Javanan Barbershop in the city of Ben. Since the cow leg and hair were already discarded and not directly sourced from individuals, no ethical considerations were required for this process.

Data availability

The supporting data for this article are provided as part of the ESI† and are accessible alongside the article. Additionally, the data that support the findings of this study are available from the corresponding author upon reasonable request. Any specific datasets or additional materials can be shared through formal communication for further verification or research purposes.

Conflicts of interest

There are no conflicts to declare.

References

1 Y. Wu, N. Ailijiang, Y. Cui, Z. Abdusalam, Y. Wu, J. Ma, et al., Removal of mixed antibiotics from saline wastewater under intermittent electrical stimulation and alterations of microbial communities and resistance genes, Environ. Res., 2025, **268**, 120772. Available from: https://linkinghub.elsevier.com/retrieve/pii/S0013935125000234.

2 H. Befenzi, A. Ezzariai, J. Baghor, H. Arrach, J. Armengaud, M. Kielbasa, et al., Bjerkandera adusta TM11 for the bioremediation of fluoroquinolone antibiotics spiked in wastewater: A sustainable approach to pharmaceutical contaminant biotransformation, Ecotoxicol. Environ. Saf., 2025, **291**, 117898. Available from: https://linkinghub.elsevier.com/retrieve/pii/S0147651325002349.

3 L.-K. Qiao, L.-Y. He, F.-Z. Gao, Z. Huang, H. Bai, Y.-C. Wang, et al., Deciphering key traits and dissemination of antibiotic resistance genes and degradation genes in pharmaceutical wastewater receiving environments, Water Res., 2025, **275**, 123241. Available from: https://linkinghub.elsevier.com/retrieve/pii/S0043135425001551.

4 N. Wang, Y. Yang, C. Gong, X. Liu, K. Wang, W. He, et al., Study of Fe/Cu composite Fenton-like catalyst in the treatment of antibiotic wastewater: Preparation, application, degradation pathways and working mechanism, J. Environ. Chem. Eng., 2025, **13**(2), 115926. Available from: https://linkinghub.elsevier.com/retrieve/pii/S2213343725006220.

5 N. Li, M. Li, P. Chen, A. Wood, J. Hilton, Q. Zhou, et al., Mapping bacterial diversity and antibiotic resistance across wastewater treatment plant stages: Insights from high-resolution 16S rRNA sequencing of the V3-V4 regions to detection of multi-drug resistant bacteria, J. Water Process Eng., 2025, **71**, 107143. Available from: https://linkinghub.elsevier.com/retrieve/pii/S2214714425002156.

6 R. Zhang, X. Chen, Y. Li, H. Tan, W. Huang, L. Li, et al., Removal of antibiotic resistance from wastewater in aquatic ecosystems dominated by submerged macrophytes, J. Hazard. Mater., 2025, **489**, 137706. Available from: https://linkinghub.elsevier.com/retrieve/pii/S030438942500620X.

7 M. W. Nugraha, S. Kim, F. Roddick, Z. Xie and L. Fan, A review of the recent advancements in adsorption technology for removing antibiotics from hospital wastewater, J. Water Process Eng., 2025, **70**, 106960. Available from: https://linkinghub.elsevier.com/retrieve/pii/S2214714425000327.

8 J. Yang, S. Wang, X. Luo, Z. Yu and Y. Zhou, Fenton-like process in antibiotic-containing wastewater treatment: applications and toxicity evaluation, Chin. Chem. Lett., 2025, 110996. Available from: https://linkinghub.elsevier.com/retrieve/pii/S1001841725001822.

9 P. Mishra, G. Tripathi, V. Mishra, T. Ilyas, F. S. Irum, et al., Antibiotic contamination in wastewater treatment plant effluents: Current research and future perspectives, Environ. Nanotechnol., Monit. Manage., 2025, **23**, 101047. Available from: https://linkinghub.elsevier.com/retrieve/pii/S221515322500008X.

10 J. Wang, X. Hui, H. Liu and X. Dai, Classification, characteristics, harmless treatment and safety assessment of antibiotic pharmaceutical wastewater (APWW): A comprehensive review, Chemosphere, 2024, **366**, 143504.

Available from: https://linkinghub.elsevier.com/retrieve/pii/S0045653524024044.

11 G. Zhang, P. Ju, S. Lu, Y. Chen, Z. Chen, J. Sun, *et al.*, Efficient adsorption of antibiotics in aqueous solution through ZnCl2-activated biochar derived from *Spartina alterniflora*, *Colloids Surf., A*, 2024, **694**, 134139, DOI: 10.1016/j.colsurfa.2024.134139.

12 P. Su, Q. Huo, C. Zhang, Z. Wang and Y. Qiao, Synthesis of MIL-53(Fe) implanted carbon spheres derived from resorcinol-formaldehyde resins for fast adsorption of antibiotics: Enhanced adsorption and pH adaptability, *J. Cleaner Prod.*, 2024, **461**, 142395, DOI: 10.1016/j.jclepro.2024.142395.

13 T. He, X. Liu, S. Lv, D. Wei and L. Liu, Three-dimensional graded porous structure and compressible KGM-GO/CS/SA composite aerogel spheres for efficient adsorption of antibiotics, *Sep. Purif. Technol.*, 2024, **346**, 127547, DOI: 10.1016/j.seppur.2024.127547.

14 S. Lv, F. Rong, S. Hu, G. Wang, J. Liu, G. Hou, *et al.*, Competitive adsorption and desorption of three antibiotics in distinct soil aggregate size fractions, *Ecotoxicol. Environ. Saf.*, 2023, **259**(266), 115002, DOI: 10.1016/j.ecoenv.2023.115002.

15 E. Ameri, A. A. Beni and Z. P. Nodeh, Chinese Journal of Chemical Engineering Design and manufacture of emulsion liquid membrane based on various amine extractants for separation and extraction of succinic acid from fermentation broth, *Chin. J. Chem. Eng.*, 2023, **61**, 173–179, DOI: 10.1016/j.cjche.2023.02.012.

16 B. A. Aghababai, A. Esmaeili and Y. Behjat, Invent of a simultaneous adsorption and separation process based on dynamic membrane for treatment Zn(II), Ni(II) and, Co(II) industrial wastewater, *Arabian J. Chem.*, 2021, **14**(7), 103231, DOI: 10.1016/j.arabjc.2021.103231.

17 F. Googerdchian, A. Moheb and R. Emadi, Lead sorption properties of nanohydroxyapatite-alginate composite adsorbents, *Chem. Eng. J.*, 2012, **200–202**, 471–479, DOI: 10.1016/j.cej.2012.06.084.

18 A. A. Beni and A. Esmaeili, Fabrication of 3D hydrogel to the treatment of moist air by solar/wind energy in a simulated battery recycle plant salon, *Chemosphere*, 2020, **246**, 125725, DOI: 10.1016/j.chemosphere.2019.125725.

19 M. Haghmohammadi, N. Sajjadi, A. Aghababai, S. Mostafa, A. Nezarat and S. Delnabi, Journal of Water Process Engineering Synthesis of activated carbon/magnetite nanocatalyst for sono-Fenton-like degradation process of 4-chlorophenol in an ultrasonic reactor and optimization using response surface method, *J. Water Process Eng.*, 2023, **55**, 104216, DOI: 10.1016/j.jwpe.2023.104216.

20 A. Haghighizadeh, O. Rajabi, A. Nezarat, Z. Hajyani, M. Haghmohammadi, S. Hedayatikhah, *et al.*, Comprehensive analysis of heavy metal soil contamination in mining Environments : Impacts , monitoring Techniques , and remediation strategies, *Arabian J. Chem.*, 2024, **17**(6), 105777, DOI: 10.1016/j.arabjc.2024.105777.

21 G. Abedi, A. Jamali, A. Montazeri, Z. Hajyani, A. Nezarat and A. Aghababai, Results in Engineering Synthesis of green

ceramic adsorbent for the treatment of tire factory effluent containing lead , zinc , aluminum , cobalt , iron and manganese ions, *Results Eng.*, 2024, **23**, 102591, DOI: 10.1016/j.rineng.2024.102591.

22 A. A. Beni and A. Esmaeili, Design and optimization of a new reactor based on biofilm-ceramic for industrial wastewater treatment, *Environ. Pollut.*, 2019, **255**, 113298. Available from: https://linkinghub.elsevier.com/retrieve/pii/S026974911933979X.

23 Z. P. Nodeh, A. A. Beni and A. J. Moghadam, Development of evaporation technique for concentrating lead acid wastewater from the battery recycling plant, by nanocomposite ceramic substrates and solar/wind energy, *J. Environ. Manage.*, 2023, **328**, 116980, DOI: 10.1016/j.jenvman.2022.116980.

24 A. Aghababai Beni and H. Jabbari, Nanomaterials for Environmental Applications, *Results Eng.*, 2022, **15**, 100467, DOI: 10.1016/j.rineng.2022.100467.

25 S. A. Abdollahi, N. Mokhtariyan and E. Ameri, Design, synthesis and application of a sponge-like nanocomposite ceramic for the treatment of Ni(II) and Co(II) wastewater in the zinc ingot industry, *Arabian J. Chem.*, 2022, **15**(1), 103477, DOI: 10.1016/j.arabjc.2021.103477.

26 M. Messaoudi, N. Tijani, S. Baya, A. Lahnafi, H. Ouallal, H. Moussout, *et al.*, South African Journal of Chemical Engineering Characterization of ceramic pieces shaped from clay intended for the development of filtration membranes, *S. Afr. J. Chem. Eng.*, 2021, **37**, 1–11, DOI: 10.1016/j.sajce.2021.03.004.

27 B. Achiou, H. Elomari, A. Bouazizi, A. Karim, M. Ouammou, A. Albizane, *et al.*, Manufacturing of tubular ceramic microfiltration membrane based on natural pozzolan for pretreatment of seawater desalination, *Desalination*, 2017, **419**, 181–187, DOI: 10.1016/j.desal.2017.06.014.

28 L. C. Hwa, M. B. Uday, N. Ahmad, A. M. Noor, S. Rajoo and B. Zakaria K, Integration and fabrication of the cheap ceramic membrane through 3D printing technology, *Mater. Today Commun.*, 2018, **15**, 134–142, DOI: 10.1016/j.mtcomm.2018.02.029.

29 S. Saja, A. Bouazizi, B. Achiou, H. Ouaddari, A. Karim, M. Ouammou, *et al.*, Fabrication of low-cost ceramic ultrafiltration membrane made from bentonite clay and its application for soluble dyes removal, *J. Eur. Ceram. Soc.*, 2020, **40**(6), 2453–2462, DOI: 10.1016/j.jeurceramsoc.2020.01.057.

30 S. Lan, P. Shen, Q. Zheng, L. Qiao, L. Dong and D. Liu, Effective flotation separation of apatite from dolomite using a new eco-friendly depressant gallic acid, *Green Chem.*, 2024, **26**(3), 1627–1636. Available from: https://xlink.rsc.org/?DOI=D3GC03325B.

31 L. Jing, L. Xu, K. Xue, D. Wang, Z. Ma, J. Meng, *et al.*, Selective depression by using environment-friendly depressant pectin in apatite and dolomite flotation system, *Miner. Eng.*, 2023, **203**, 108373. Available from: https://linkinghub.elsevier.com/retrieve/pii/S0892687523003874.

32 H. Noukrati, Y. Hamdan, O. Marsan, R. El Fatimy, S. Cazalbou, C. Rey, *et al.*, Sodium fusidate loaded apatitic

calcium phosphates: Adsorption behavior, release kinetics, antibacterial efficacy, and cytotoxicity assessment, *Int. J. Pharm.*, 2024, **660**, 124331. Available from: https://linkinghub.elsevier.com/retrieve/pii/S0378517324005659.

33 H. Ait Said, H. Elbaza, M. Lahcini, A. Barroug, H. Noukrati and H. Ben Youcef, Development of calcium phosphate-chitosan composites with improved removal capacity toward tetracycline antibiotic: Adsorption and electrokinetic properties, *Int. J. Biol. Macromol.*, 2024, **257**, 128610. Available from: https://linkinghub.elsevier.com/retrieve/pii/S0141813023055095.

34 Y. Yan, Y. Deng, W. Li, W. Du, Y. Gu, J. Li, *et al.*, Phytoremediation of antibiotic-contaminated wastewater: Insight into the comparison of ciprofloxacin absorption, migration, and transformation process at different growth stages of *E. crassipes*, *Chemosphere*, 2021, **283**, 131192. Available from: https://linkinghub.elsevier.com/retrieve/pii/S0045653521016647.

35 A. Vancsik, L. Szabó, L. Bauer, Z. Pirger, M. Karlik, A. C. Kondor, *et al.*, Impact of land use-induced soil heterogeneity on the adsorption of fluoroquinolone antibiotics, tested on organic matter pools, *J. Hazard. Mater.*, 2024, **474**, 134704, DOI: 10.1016/j.jhazmat.2024.134704.

36 P. Hu, Y. Dou, B. Ji, M. Miao, Y. Li and T. Hao, Chlorination-improved adsorption capacity of microplastics for antibiotics: A combined experimental and molecular mechanism investigation, *J. Hazard. Mater.*, 2024, **467**, 133734, DOI: 10.1016/j.jhazmat.2024.133734.

37 S. M. Lee, J. G. Kim, W. G. Jeong, D. S. Alessi and K. Baek, Adsorption of antibiotics onto low-grade charcoal in the presence of organic matter: Batch and column tests, *Chemosphere*, 2024, **346**, 140564, DOI: 10.1016/j.chemosphere.2023.140564.

38 C. Mejías, J. Martín, J. L. Santos, I. Aparicio and E. Alonso, Implications of polystyrene and polyamide microplastics in the adsorption of sulfonamide antibiotics and their metabolites in water matrices, *Aquat. Toxicol.*, 2024, **271**, 106934, DOI: 10.1016/j.aquatox.2024.106934.

39 W. A. Khanday, M. J. Ahmed, P. U. Okoye and E. H. Hummadi, Single-step H3PO4 activation of chitosan

for efficient adsorption of amoxicillin and doxycycline antibiotic pollutants, *Inorg. Chem. Commun.*, 2025, **175**, 114189. Available from: https://linkinghub.elsevier.com/retrieve/pii/S138770032500303X.

40 S. Hu, L. Tang, R. Zhang, R. Sun, Y. Zhang, Z. Song, *et al.*, An amino-functionalized magnetic mesoporous silica nano-adsorbent for removing antibiotics from aqueous environments, *J. Water Process Eng.*, 2025, **71**, 107248. Available from: https://linkinghub.elsevier.com/retrieve/pii/S2214714425003204.

41 A. Esmaeili and A. A. Beni, A novel fixed-bed reactor design incorporating an electrospun PVA/chitosan nanofiber membrane, *J. Hazard. Mater.*, 2014, **280**, 788–796.

42 A. A. Beni and A. Esmaeili, Environmental Technology & Innovation Biosorption , an efficient method for removing heavy metals from industrial effluents : A Review, *Environ. Technol. Innovation*, 2020, **17**, 100503, DOI: 10.1016/j.eti.2019.100503.

43 H. D. Tamaguelon, V. O. Shikuku, S. Tome, F. G. Titini, P. Ondiek, T. Strothmann, *et al.*, Unary adsorption of sulfonamide antibiotics onto pozzolan-tyre ash based geopolymers: Isotherms, kinetics and mechanisms, *Chem. Eng. Res. Des.*, 2024, **206**, 40–52, DOI: 10.1016/j.cherd.2024.05.009.

44 Z. Wu, Z. Guo, D. Dong, F. Wu, J. Li and X. Yang, Distinguishable adsorption interaction of virgin and biofilm covered polyethylene and polylactic acid for antibiotics, *J. Environ. Chem. Eng.*, 2023, **11**(6), 111143, DOI: 10.1016/j.jece.2023.111143.

45 X. Xu, Y. Weng, J. Zhuang, H. Pei, B. Wu, W. Wu, *et al.*, Enhanced adsorption capacity of antibiotics by calamus-biochar with phosphoric acid modification: Performance assessment and mechanism analysis, *J. Taiwan Inst. Chem. Eng.*, 2024, **161**, 105541, DOI: 10.1016/j.jtice.2024.105541.

46 A. Haghighizadeh, A. Aghababai Beni, M. Haghmohammadi, M. S. S. Adel and S. Farshad, Green Synthesis of ZnO-TiO2 Nano-Photocatalyst Doped with Fe(III) Ions Using Bitter Olive Extract to Treat Textile Wastewater Containing Reactive Dyes, *Water, Air, Soil Pollut.*, 2023, **234**(6), 1–17, DOI: 10.1007/s11270-023-06374-w.